

Research Paper

Prediction and optimization of radiative thermal properties of ultrafine fibrous insulations

Jianming Yang^a, Huijun Wu^{a,*}, Moran Wang^b, Shiquan He^a, Huakun Huang^a^a College of Civil Engineering, Guangzhou University, Guangzhou 510006, China^b Department of Engineering Mechanics, Tsinghua University, Beijing 100084, China

HIGHLIGHTS

- Radiative thermal conductivities of ultrafine fibrous insulations were predicted.
- Infrared optical constants of ultrafine fibrous insulations were determined.
- Critical diameter of PVDF fibrous insulations was deduced with 1.06 μm .
- Fiber diameters were optimized for minimum radiative thermal conductivity.
- Optimized radiative thermal conductivity is 25% lower than that by as-prepared.

ARTICLE INFO

Article history:

Received 8 December 2015

Revised 15 April 2016

Accepted 9 May 2016

Available online 10 May 2016

Keywords:

Thermal insulations

Radiative thermal conductivity

Ultrafine fiber

Fiber diameter

Optimization

ABSTRACT

Predicting and optimizing radiative thermal properties have been acknowledged as an efficient way to improve thermal insulation performance of fibrous materials with high porosity. Based on experimental investigation of infrared spectral of ultrafine fibrous insulations with diameters of 520–650 nm, a method of calculating radiative thermal properties was presented by combining Rosseland equation, Mie scattering theory, Beer's law and Subtractive Kramers–Kronig (SKK) relation. To ensure the calculation correct the uniqueness analysis was performed for Poly(vinylidene fluoride) (PVDF) fibers, which indicated the valid fiber diameter was less than 1.06 μm . The calculated thermal radiative conductivities by using the method agreed well with the measured data. The effect of fiber diameter on the thermal properties of the fibrous insulations was also investigated to minimize the radiative thermal conductivity. The results indicated that the minimized radiative thermal conductivities by regulating fiber diameters could be approximately 25% smaller than those for experimental fiber diameters. The method of predicting and minimizing radiative thermal conductivities of fibrous insulations demonstrated in this paper could be of great advantage to thermal engineering applications aiming to reducing heat loss and saving energy.

© 2016 Elsevier Ltd. All rights reserved.

0. Introduction

Fibrous materials with low thermal conductivity and high porosity have widely been used as thermal insulations [1] so as to reduce heat loss in aerospace crafts, industrial equipment, building construction [2] and textiles [3]. Owing to the high porosity (commonly greater than 80%) of fibrous insulations [4], the radiative thermal flux may be acknowledged as an important part of the total heat flux within fibrous insulations (e.g. superfine polyvinyl alcohol textiles [5] and metallic foams [6]). The radiative thermal flux in lightweight fibrous insulations could be up to 30% [7] of

the total heat flux even at moderate temperatures (300–400 K). Therefore, reducing the radiative heat flux is an efficient way to improve the thermal insulation performance of fibrous material with high porosity.

Extensive investigations have been conducted on decreasing the radiative thermal conductivity of the fibrous insulations [8,9]. With given optical constants of fibers, numerical method predicting the minimum effective thermal conductivity by optimizing the structure parameters (e.g. diameter, volume fraction [10]) of fibrous insulations was one of the most important approach. In the numerical method the spectral optical constants (m_i) of fibers are the fundamental data [11] to calculate thermal radiative conductivities of fibrous insulations. The spectral optical constants are constituted by real part n_i (viz., spectral refractive index) [12] and imaginary part κ_i (viz., spectral absorption index) [13], which indicates the

* Corresponding author.

E-mail address: wuhuijun@tsinghua.org.cn (H. Wu).

scattering and absorption capability of fibrous insulations, respectively [14].

However, it is very difficult or extremely time-consuming to experimentally measure the spectral optical constants of fibers for each wavelength in the whole infrared spectrum generally in infrared wavelengths (λ) of 2.5–25 μm . In fact the data of the spectral optical constants of fibrous insulations were extremely insufficient besides several specific data in few separate wavelengths. Therefore, the efforts on exploring spectral optical constants of fibrous insulations are needed to predict and optimize thermal insulation performance.

In the past few years, a method by combining experimental infrared transmittances and thermal radiation model had been reported to calculate the optical constants of particles in some certain wavelengths, such as Bhattacharyya et al. [15] for $\text{Zn}_{1-x}\text{Mg}_x\text{O}$ films in 0.4–0.8 μm , Gushterova and Sharlandjiev [16] for GeSe films in 0.4–1.2 μm and Dombrovsky for ceramic microspheres et al. [17] in 2.6–18 μm . Very recently Ruan et al. [18] calculated spectral optical constants of spherical particles in wide wavelengths of 2.5–25 μm by combining spectral transmittances, Mie scattering theory and SKK relations. The calculated results of optical constants were found to be feasible as the diameter of the spherical particles was smaller than the critical diameter of 1–2 μm by performing uniqueness analysis. Similarly, a certain critical diameter of fibers may exist to calculate the optical constants. As a comparison the commonly used fibers in fibrous insulations had the diameters of several dozen micrometers which were much greater than the critical fiber diameter. Herein, the previous numerical method may not be feasible for the commonly used fibrous insulations.

Recently new-type fibrous materials with finer diameters have successfully been prepared by using the newly developed micro and nano technology. Electrospinning is one of the most attractive nanotechnologies to fabricate ultrafine fibrous materials [19]. By engineering electrospinning parameters [20] the electrospun fiber diameters could be regulated from 10 nm to 10 μm [21]. Herein, electrospun fibers have well acknowledged as a type of ultrafine fibers with diameters smaller than 10 μm , which are much finer than the commonly used fibers with diameters of several dozen micrometers. The electrospun ultrafine fibers provides a possibility to calculate the unique optical constant of materials by combining experimental infrared transmittance and thermal radiation model.

Therefore, this paper was aiming to obtain the spectral optical constants of fibrous insulations with ultrafine diameters by using the numerical method combining experimental infrared transmittance and thermal radiation model. Firstly, ultrafine fibrous insulations were experimentally fabricated by using electrospinning. The spectral transmittance of the as-fabricated ultrafine fibrous insulations were experimentally investigated. Concerning the experimental results, the optical constants of fibrous insulations were then calculated by using the radiation model and SKK relation. Uniqueness analysis to ensure the calculation correct was performed and the calculated results were validated with the experimental measurements. Eventually, effect of fiber diameters on thermal conductivities were explored so as to minimize thermal conductivity by optimizing fiber diameters for improving thermal insulation performance.

1. Theoretical model of radiative thermal conductivity

1.1. Radiative thermal properties of fibrous insulations

Taking ultrafine Poly(vinylidene fluoride) (PVDF) fibers as an example of fibrous materials their microstructure characterized scanning electronic microscope (SEM) was shown in Fig. 1. The

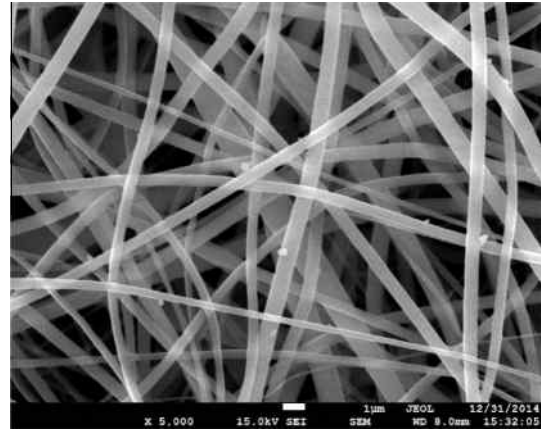


Fig. 1. SEM image of PVDF fibrous insulations.

image was obtained by a field emission scanning electron microscopy (FESEM, JSM-7001F, JEOL, Japan). The preparation process of ultrafine PVDF fibers is presented in Section 2.1. It can be observed from Fig. 1 that PVDF fibers are in infinite cylinders [22] with the ratio of length to diameter greater than 100 and ultrafine diameters (d) of 0.2–1.0 μm . The directions of their axis are randomly distributed in plane. Fig. 2 shows the scattering geometry of a PVDF fiber with incident radiation. The inclination angle (ϕ) describes the extent of the fiber direction deviating from the radiation heat flux direction. As the plane of the fiber axis is perpendicular to the direction of radiation heat flow, ϕ equals to 0.

Extinction efficiency ($Q_{e\lambda}$) is a non-dimensional and temperature-independent parameter indicating the ability of absorbing and scattering the light as the light goes through fibrous insulation. It can be calculated by Mie scattering theory [23] for infinite cylindrical fibers

$$Q_{e\lambda} = \frac{1}{x} \text{Re} \left[(a_{0\pi} + b_{0i}) + 2 \sum_{n=1}^{\infty} (a_{n\pi} + b_{ni}) \right] \quad (1)$$

where Re is the symbol of real part, $x = \pi d/\lambda$ is the size factor, a_n and b_n are Mie coefficients. As the radiation heat flux vertically incidence on infinite cylinder fibers Mie coefficients can be expressed as

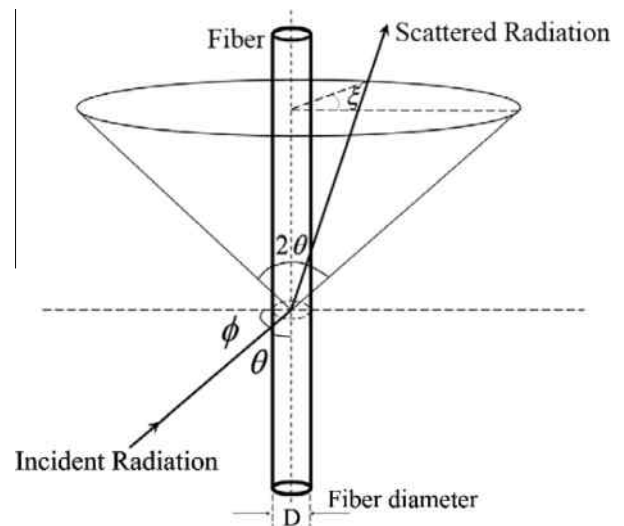


Fig. 2. Scattering geometry for a fiber with incident radiation.

$$a_{n\Pi} = \frac{[D_n(mx)/m + n/x]J_n(x) - J_{n-1}(x)}{[D_n(mx)/m + n/x]H_n^{(1)}(x) - H_{n-1}^{(1)}(x)} \quad (2)$$

$$b_{nI} = \frac{[mD_n(mx) + n/x]J_n(x) - J_{n-1}(x)}{[mD_n(mx) + n/x]H_n^{(1)}(x) - H_{n-1}^{(1)}(x)} \quad (3)$$

where J_n is the Ricatti–Bessel function of the first kind, $H_n^{(1)} = J_n + i \cdot Y_n$ is the first Ricatti–Hankel function, Y_n is the Bessel function of the second kind, J'_n and $H_n^{(1) \prime}$ are the derivatives, and D_n is the recurrence relation.

As PVDF fibers are infinite cylinders and vertical to the radiation heat flux, the extinction coefficient ($\beta_{e\lambda}$) can be expressed as [24]

$$\beta_{e\lambda} = 4Q_{e\lambda}f_v/\pi d \quad (4)$$

where f_v is the fiber volume fraction of fibrous insulation. The mean extinction coefficient (β_{eT}), indicates the temperature-dependent average extinction capability of fibrous insulation, expressed as [25]

$$\beta_{eT} = \left(\int_0^\infty \frac{1}{\beta_{e\lambda}} \frac{\partial E_{b\lambda}}{\partial E_b} d\lambda \right)^{-1} \quad (5)$$

As fibrous insulation is optically thick, the corresponding temperature-dependent radiative thermal conductivity is expressed as [11]

$$k_r = \frac{16n_T^2\sigma T^3}{3\beta_{eT}} \quad (6)$$

where T is the temperature, σ is the Stefan–Boltzmann constant, and n_T is temperature-depended effective refractive index of composite. Considering the relation between temperature and wavelength, the transformation is made as follow [10]

$$n_T = \left(\int_0^\infty \frac{1}{n_{c,\lambda}} \frac{\partial E_{b\lambda}}{\partial E_b} d\lambda \right)^{-1} \quad (7)$$

where $n_{c\lambda}$ is the spectral refractive index of composite, which can approximate be calculated by $n_{c\lambda} = \sum_{i=1}^m n_{i\lambda}f_i$, where $n_{i\lambda}$ is spectral refractive index of component i , and f_i is the volume fraction of component i .

During the calculation of radiative thermal properties, the wavelengths used were in the range of 2.5–25 μm while the fiber diameters were in the range of 0.5–5 μm . It is possible that the wavelengths are smaller or greater than fiber diameters. Whatever the wavelengths are smaller or greater than fiber diameters, the thermal radiation model based on Mie theory and Rosseland equation above is feasible [11].

1.2. Determination of optical constants of PVDF fibrous insulations

1.2.1. Theoretical method by establishing equations

Ignoring scattering radiation between fibers the spectral extinction coefficient of fibrous insulations can be calculated by the Beer's law [26]

$$\beta_{e\lambda,\tau} = -\ln(\tau_\lambda)/L \quad (8)$$

Combined with Eq. (4), the spectral extinction efficiency can be determined by

$$Q_{e\lambda,\tau} = -\frac{\pi d \ln(\tau_\lambda)}{4L f_v} \quad (9)$$

where L is thickness of the PVDF fibrous sample, and τ_λ is the experimental infrared spectral transmittances. Combined with Eq. (1), the spectral refractive index n_λ and spectral absorption index κ_λ could be calculated.

Beside the above equation, the other equation of n_λ and κ_λ can be provided by SKK relation [18]

$$n(\lambda) = n(\lambda_m) + \frac{2(\lambda_m^2 - \lambda^2)}{\pi} P \int_0^\infty \frac{\lambda_0 \kappa(\lambda_0)}{(\lambda^2 - \lambda_0^2)(\lambda_m^2 - \lambda_0^2)} d\lambda_0 \quad (10)$$

where λ_m is the reference wavelength of PVDF materials. During the calculation, $\lambda_m = 0.5 \mu\text{m}$ and $n(\lambda_m) = 1.41$.

The spectral optical constants of fibrous insulations can be obtained by solving the equations.

1.2.2. Uniqueness analyses of solution

Because of complex scattering amplitude function in the Mie scattering theory, a certain value of $Q_{e\lambda}$ may correspond to a series of n_λ and κ_λ . In other words, multiple solutions of n_λ and κ_λ may simultaneously satisfy the transmittance at each wavelength. However, since n_λ and κ_λ of PVDF fibers are unique the uniqueness analysis of solutions for n_λ and κ_λ must be performed to ensure the calculation correct.

For spherical particles, Milham et al. [27] and Ruan et al. [14] performed uniqueness analysis by determining valid uniqueness region of $x_{\min} \leq x \leq x_{\max}$ for size factor x for each n_λ and κ_λ . Similarly for infinite cylinder fibers, uniqueness analysis was performed as follows.

- (a) For a given n , the relationship between $Q_{e\lambda}$ and x under different κ_λ values is shown in Fig. 3(a). There are two critical values $x_{l,n}$ and $x_{u,n}$ corresponding to each n value. Where $x_{l,n}$ represents the lower limit, which is commonly

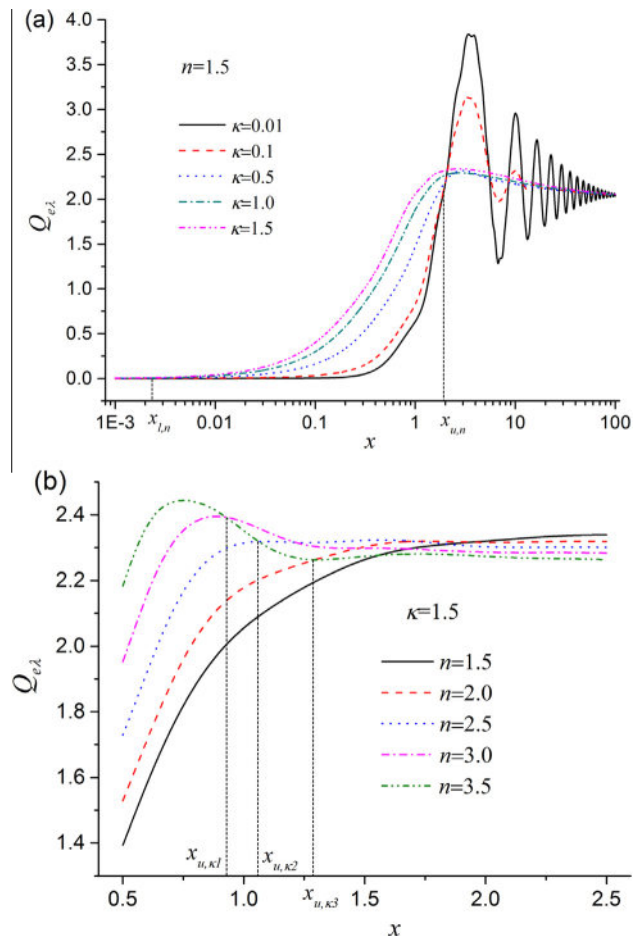


Fig. 3. Relation between extinction efficiency and size factor. (a) For a given n ; (b) for a given κ .

significantly less than the calculated range of size factor [14]. $x_{u,n}$ is the upper limit and can be obtained by the condition expression

$$[Q(\kappa_1, x) - Q(\kappa_2, x)] \cdot [Q(\kappa_1, x + dx) - Q(\kappa_2, x + dx)] > 0 \quad (11)$$

where κ_1 and κ_2 represent any values. $x_{u,n}$ is the value eventually satisfy the equation as x is increased. Thus, the uniqueness of solutions can be assured when $x \leq x_{u,n}$. Otherwise a serious multi-valued feature is shown in Fig. 3(a).

(b) For a given κ , the relationship between $Q_{e,\lambda}$ and x under different n_λ values is shown in Fig. 3(b). It can be observed that there is a upper limit $x_{u,\kappa}$ corresponding to each κ value for a given range of n , such as $x_{u,\kappa1}$ for n of 1.5–3.5, $x_{u,\kappa2}$ for n of 1.5–3.0 and $x_{u,\kappa3}$ for n of 1.5–2.5. Similarly, $x_{u,\kappa}$ can be obtained by the condition expression

$$[Q(n_1, x) - Q(n_2, x)] \cdot [Q(n_1, x + dx) - Q(n_2, x + dx)] > 0 \quad (12)$$

where n_1 and n_2 represent any values in the given region of n . $x_{u,\kappa}$ is the value eventually satisfy Eq. (12) as x is increased. Thus, the uniqueness of solutions can be assured when $x \leq x_{u,\kappa}$. Otherwise a serious multi-valued feature is show in Fig. 3(b).

Therefore, once all the predicted n_λ and κ_λ satisfy the one of two uniqueness solution region (viz., $x \leq x_{u,n}$ and $x \leq x_{u,\kappa}$), the solutions for n_λ and κ_λ are unique and valid.

2. Experimental

2.1. Preparation of ultrafine fibrous insulations by electrospinning

Ultrafine PVDF fibers were prepared by using electrospinning technology. Firstly, PVDF solution with concentration of 28 wt.% was prepared by dissolving PVDF particles (melting point of 445 K, Baishi Co. Ltd., China) in N,N-dimethyl-formamide (>98%, DMF, Baishi Co. Ltd., China) under magnetic stirring for 0.5 h at 60 °C and then cooled to room temperature with continuous stirring. The PVDF solution was then electrospun by using an electrospinning apparatus (Model: NEU, Kato Tech Co. Ltd., Japan). Fig. 4 illustrates the electrospinning process of PVDF. Ultrafine PVDF fibrous insulations were obtained on the roller collection. The detailed electrospinning process could be found in our previous work [28].

Three samples of PVDF fibrous insulations (#1–#3) with different fiber diameters were prepared by regulating electrospinning voltage (viz., 15, 17.5 and 20 kV, respectively). The electrospun PVDF sample #1 was used for the calculation of optical constants of the PVDF fibers. The other samples #2 and #3 were used to validate the calculated results by using the numerical method.

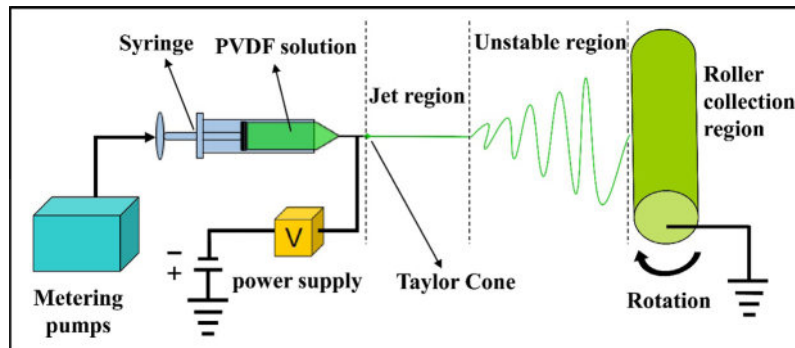


Fig. 4. Schematic of electrospinning for ultrafine PVDF fibers.

2.2. Microstructure of ultrafine fibrous insulations

The thickness (L) of the three samples (#1–#3) was measured by using a thickness gauge (0–10 mm, Chen Lu Co. Ltd., China). The thicknesses were obtained by averaging five different positions. The volume density, $\rho = M/V$, where V is volume of sample and M is the mass measured by Electronic analytical balance (Sartorius BP211D, Germany). The volume fraction was correspondingly calculated by ρ/ρ_0 , where the bulk density (ρ_0) of PVDF material is 1.78 g cm⁻³.

Fig. 5(a) shows the SEM image of sample #1, and the corresponding diameter distribution as shown in Fig. 5(b) was determined by concerning 50 fibers, by using the Nano-measure software. It can be observed that the diameters vary in 0.3–0.9 μm. It can also be fitted by Gaussian distribution with average diameter (d) of 0.52 μm and standard deviation (σ) of 0.096 μm.

2.3. Infrared spectral transmittances of ultrafine fibrous insulations

FTIR spectrometer (Tensor27, Bruker, Germany) was used to investigate infrared spectral transmittances of the electrospun PVDF fibrous insulations #1 under the wavelength of 2.5–25 μm. Fig. 6(a) illustrates the measuring process of the infrared spectral transmittances. A testing PVDF sample with size of 2.0 × 2.0 cm² was first prepared and then stuck on the aluminum plate containing a circular hole with diameter of 1.6 cm. Before testing, the measurement of the blank aluminum plate was to eliminate environmental effects including H₂O, CO₂ and temperature.

The transmittance is the ratio of the intensity transmitted through the sample (I_λ) to the incident intensity ($I_{0,\lambda}$), that is, $\tau_\lambda = I_\lambda/I_{0,\lambda}$. The infrared spectral transmittance of sample #1 was obtained by averaging two measurements at the front and reverse sides as shown in Fig. 6(b). The occurrence of bands at 445, 510, 614, 764, 840 and 976 cm⁻¹ indicates the presence of a mixture crystalline phase α and β for electrospun PVDF fibrous insulations [29].

2.4. Calculation of radiative thermal conductivity from experimental transmittance

Based on the measured infrared spectral transmittances of the PVDF insulations, the extinction coefficient ($\beta_{e,\lambda,\tau}$) can be obtained by the Beer's Law in Eq. (8). Under the assumption that the fibrous insulation adsorbs and scatters isotropically, the Rosseland approximation can be used to calculate the Rosseland mean extinction coefficient [30]

$$\beta_{eT,\tau} = \left(\int_0^\infty \frac{1}{\beta_{e,\lambda,\tau}} \frac{\partial E_{b\lambda}}{\partial E_b} d\lambda \right)^{-1} \quad (13)$$

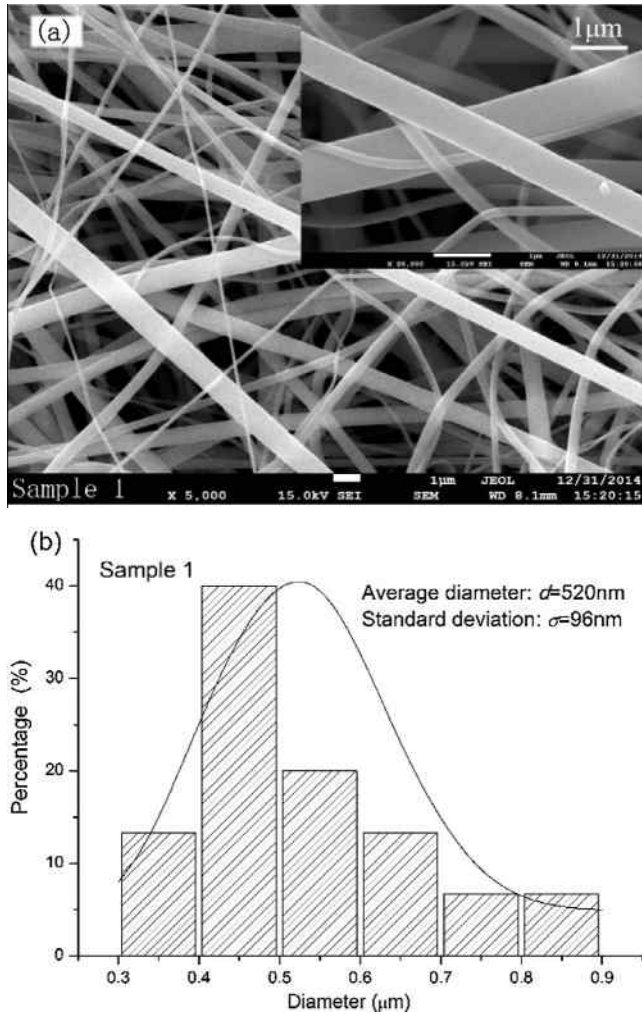


Fig. 5. Size characterization of ultrafine PVDF fibers for sample #1. (a) SEM image; (b) fiber diameter distribution.

In practical application, PVDF fibrous insulation is optically thick. The radiative thermal conductivity can be calculated by Rosseland equation [30]

$$k_{r,\tau} = \frac{16\sigma T^3}{3\beta_{ef,\tau}} \quad (14)$$

3. Numerical calculation and uniqueness analysis of optical constants

3.1. Calculation and validation with experimental results

The optical constants of PVDF fibers for wavelengths of 2.5–25 μm were calculated using Eqs. (9) and (10), shown in Fig. 7. Large fluctuation of optical constants appeared for various wavelengths. It indicated that the absorption and refractive index of fibrous insulations were significantly different for various wavelengths. The absorption and refractive index are intrinsic parameters of materials, and their values for each wavelength were dependent upon the functional groups of the materials [31].

Based on the calculated optical constants of sample #1, the infrared spectral transmittances of samples #2 and #3 were calculated by Eqs. (1) and (9) as shown in Fig. 8. Compared to

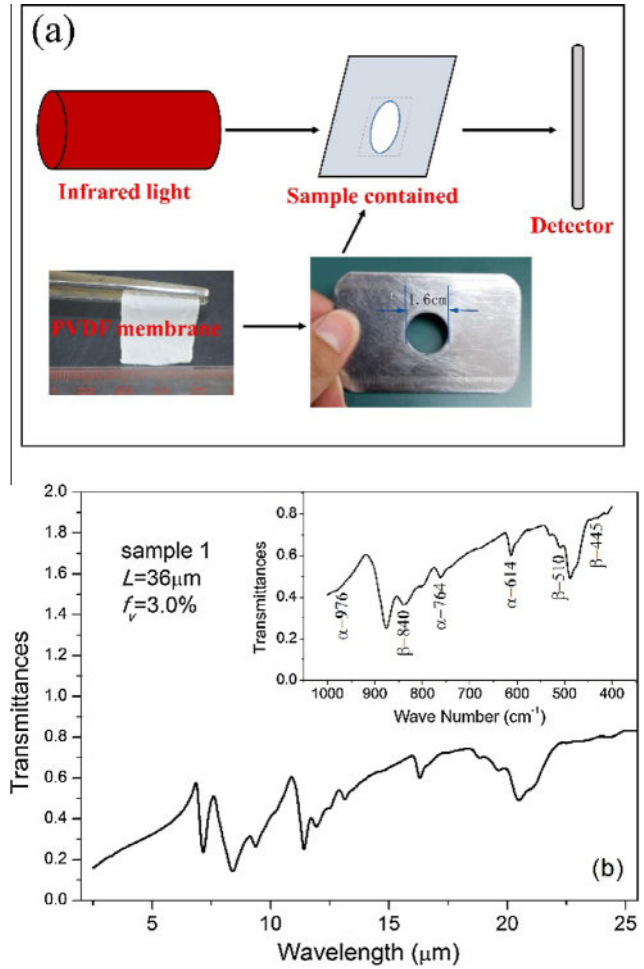


Fig. 6. Experimental investigation of infrared spectral transmissions. (a) Measuring process; (b) transmittances of electrospun PVDF fibrous insulations.

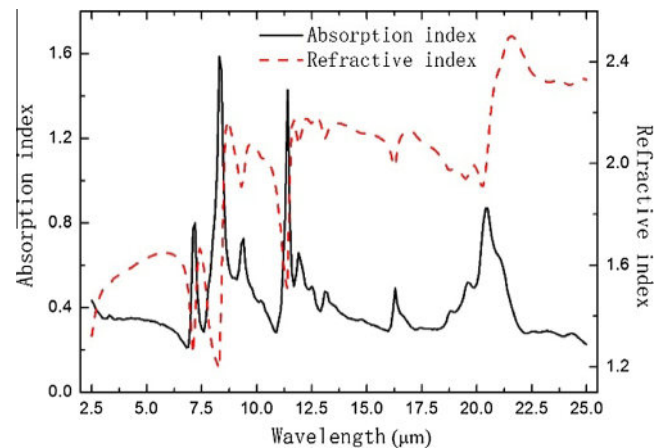


Fig. 7. Optical constants of electrospun PVDF fibrous insulations.

the experimentally measured results by using FTIR spectrometer, the predicted ones by theoretical method agreed well although little deviation existed. The little deviations mainly occurred at wavelengths of 12–25 μm (viz., spectrums of 900–400 cm^{-1}), which attributes to the mixing of different crystalline owing to electrospinning instability [20].

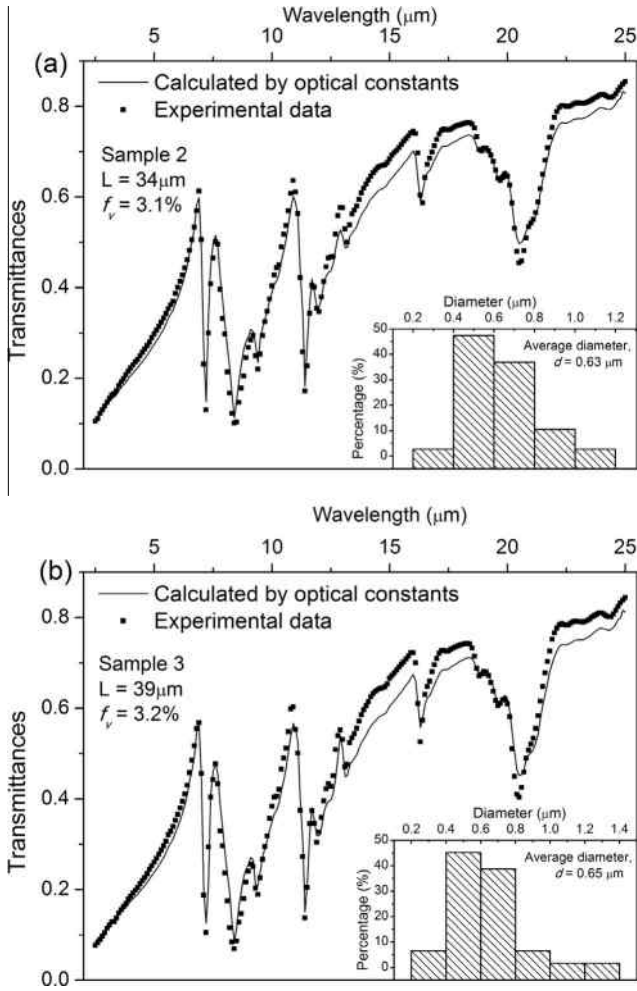


Fig. 8. Comparison of calculated and measured transmittances for different samples. (a) Sample #2; (b) sample #3.

3.2. Uniqueness analysis of solutions

During the calculation of optical constants, the size factor $x_{u,n}$ was determined and shown in Fig. 9(a). The area A below the size factor curve was the unique and valid region for any κ_λ values. Since the calculated λ of 2.5–25 μm and d of 0.52 μm , the involved x ($x = \pi d/\lambda$) was 0.065–0.65. Considering the range of predicted n_λ of PVDF was 1.20–2.50, the minimum $x_{u,n}$ of 0.338 appeared at n_λ of 2.50. Therefore, the solutions for n_λ and κ_λ in x of 0.065–0.338 corresponding to λ of 4.84–25 μm were unique. As a comparison the solutions in λ of 2.5–4.84 μm (i.e., n_λ of 1.32–1.62) required further validation.

The size factor $x_{u,\kappa}$ was determined and shown in Fig. 9(b). Below the $x_{u,\kappa}$ curve (viz., area B) was the unique solution for any n_λ of 1.32–1.62. $x_{u,\kappa}$ appears infinite at κ_λ of 0.52–1.0, which indicates unique solutions of n_λ and κ_λ as κ is a value between 0.52 and 1.0 and n is a value between 1.32 and 1.62. Considering λ of 2.5–4.84 μm was corresponding to the κ_λ of 0.34–0.43 μm , which corresponds to the x of 0.338–0.65, obviously smaller than the $x_{u,\kappa}$ of 3.3. Thus, the solutions for n_λ and κ_λ in λ of 2.5–4.84 μm are unique.

Therefore, all the predicted n_λ and κ_λ of PVDF fibers are unique.

3.3. Critical diameter for uniqueness solution

Critical diameter (d_c) was defined as a critical value when the solutions of n_λ and κ_λ eventually satisfy the uniqueness as d is

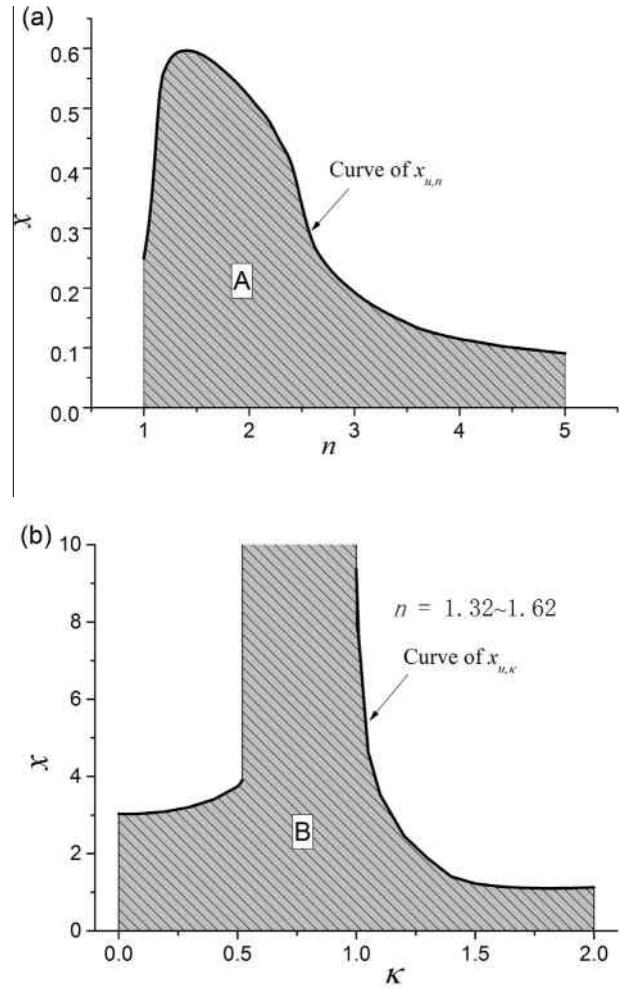


Fig. 9. Area of unique solutions region. (a) Area A for relation between $x_{u,n}$ and n ; (b) area B for relation between $x_{u,\kappa}$ and κ .

increased. The calculation of m_λ would be feasible only if d was less than d_c . Obviously, d_c appeared when $x \leq x_{u,n}$ and $x \leq x_{u,\kappa}$ were firstly simultaneously unsatisfied.

For n_λ of 1.2–2.5 and κ_λ of 0.21–1.59, the curves of $x_{u,n}$ and $x_{u,\kappa}$ are shown in Fig. 10(a) and (b) respectively. Below the curves were the unique solution regions (areas C and D). In addition, x for different d of 0.52, 1.0 and 1.6 μm varied with n_λ and κ_λ of PVDF fibers were presented. It can be observed from Fig. 10 that more serious x values eliminate from areas C and D with the increased fiber diameter. It can be obviously witnessed that x was always prior to be eliminated from area C than D. Thus, d_c existed as x firstly eliminated from area D with the increased d , which was determined to be 1.06 μm at κ_λ of 0.43 (viz., λ of 2.5 μm).

Therefore, the solutions n_λ and κ_λ of PVDF fibers were unique as the diameter of PVDF samples is less than d_c of 1.06 μm . It can also be deduced that the ultrafine PVDF fibers prepared by using electrospinning technology could be used to determine the optical constants by using the numerical method. This solve the problem that commonly used fibers could not satisfy the requirement of the uniqueness analysis owing to their greater fiber diameters.

4. Validation and optimization of radiative thermal conductivity

Extinction efficiencies and extinction coefficients for different diameters (e.g. 0.5, 1.5, 2.0 and 4.0 μm) were calculated using

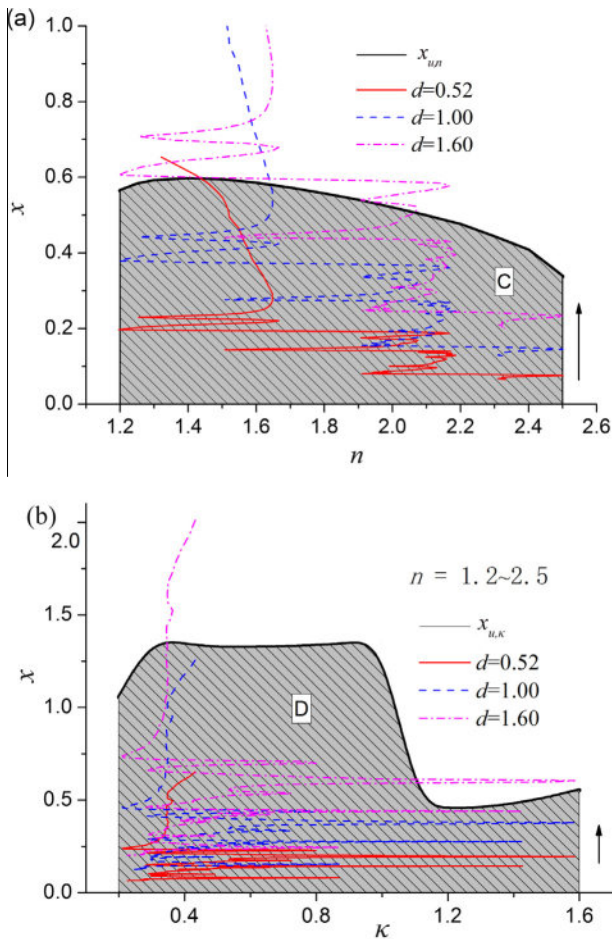


Fig. 10. Effect of fiber diameter on size factor distribution. (a) Relation between x and n ; (b) relation between x and k .

Eqs. (1)–(4), shown in Fig. 11(a) and (b) respectively. It can be observed that extinction efficiencies and extinction coefficients are significantly different for various wavelengths. The values of extinction efficiencies and extinction coefficients were obtained based on the optical constants. Therefore, they were essentially determined by the intrinsic properties of the materials. It can also be observed that fluctuation amplitudes of spectral extinction coefficient apparently decreases with the increased fiber diameter. It could be deduced by Eq. (4) that bigger diameter turns to smaller spectral extinction coefficient and even smaller fluctuation amplitude.

Based on spectral extinction coefficients, the Rosseland mean extinction coefficients for different fiber diameters could be calculated using Eq. (5) and shown in Fig. 12. It can be observed that the curve of diameter-dependent mean extinction coefficient is parabola with opening downward. The maximum mean extinction coefficient could be obtained for a certain fiber diameter (viz., optimized diameter). It may be because the mean extinction coefficient increased with the decreased diameter (several to dozens of micrometers) referring to Eqs. (4) and (5), whereas significantly decreased by forth power of diameter as the diameter turns to nanoscale according to the Rayleigh scattering theory [32] for infinite cylinders. Moreover, the optimized diameter decreased from 2.0 to 1.7 μm as the temperature was increased from 300 to 420 K. It is because the dominant wavelength (λ_{max}) turned to be smaller with the increased temperature based on Wien's energy distribution law [30]. Therefore, the optimized diameter corresponding to the maximum mean extinction coefficient would be smaller with the increased temperature.

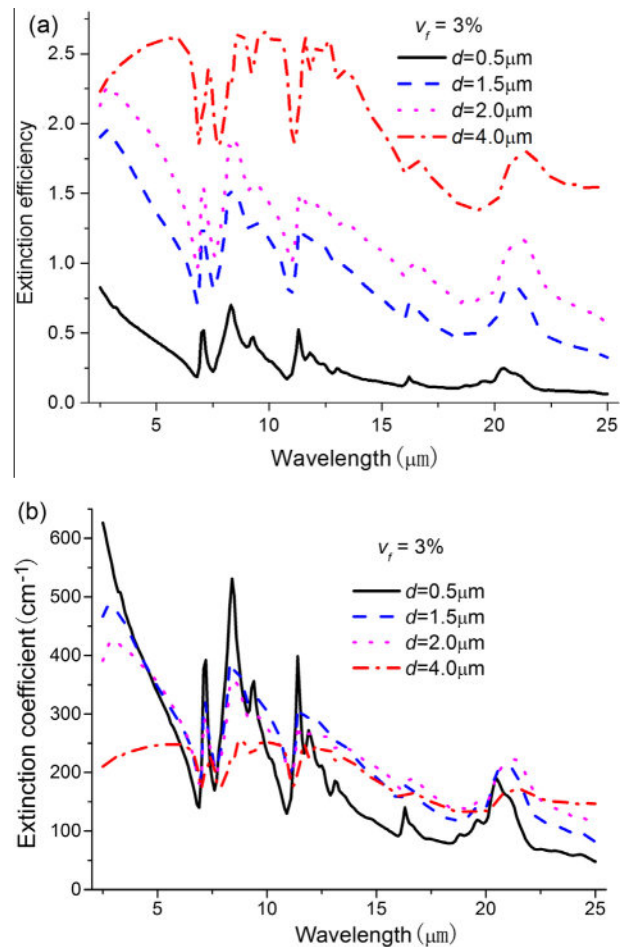


Fig. 11. Extinction efficiencies and extinction coefficients for different fiber diameters. (a) Extinction efficiency; (b) extinction coefficient.

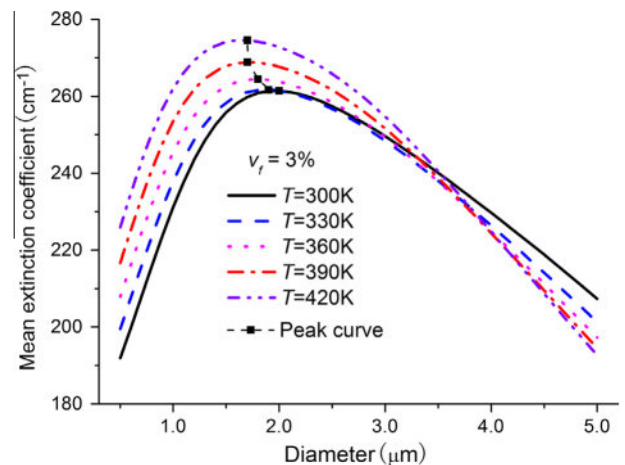


Fig. 12. Rosseland mean extinction coefficients for different fiber diameters.

Based on the Rosseland mean extinction coefficients, radiative thermal conductivities for different fiber diameters could be calculated using Eq. (6) and shown in Fig. 13. It could be observed that radiative thermal conductivities had the minimum at the optimized diameter. The trend was similar to that reported by Tong and Tien [7] with the minimum radiative thermal conductivities of the silicate and pure silica fibrous insulations at optimized diameter of 3.2 and 2.8 μm , respectively. The minimum radiative

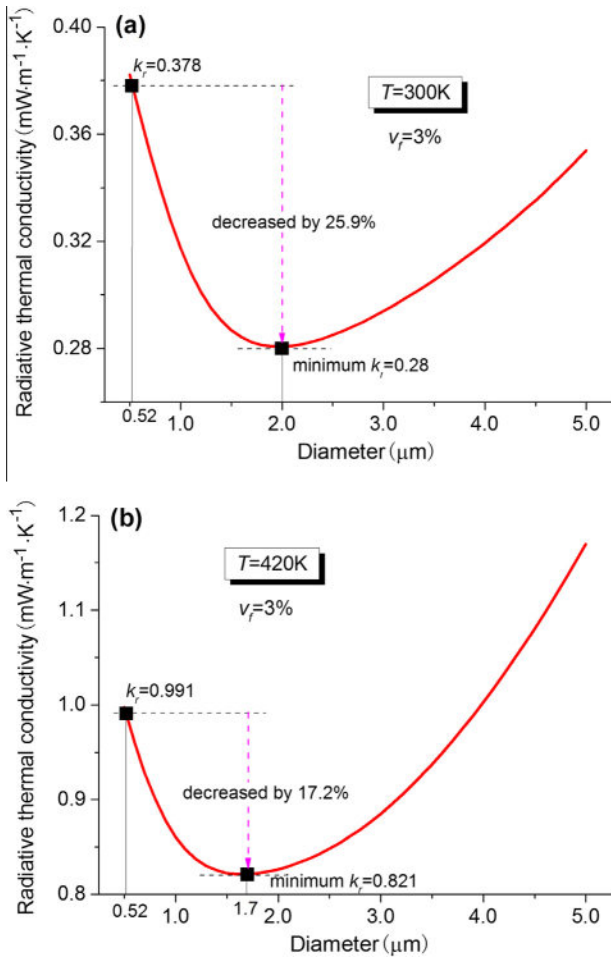


Fig. 13. Radiative thermal conductivities for different fiber diameters. (a) at 300 K; (b) at 420 K.

Table 1
Comparison of radiative thermal conductivities between experimental and optimized condition.

Sample	$k_{r,\tau}$ (mW m ⁻¹ K ⁻¹)	k_r (mW m ⁻¹ K ⁻¹)	k_{opt} (mW m ⁻¹ K ⁻¹)	$(k_{r,\tau} - k_r) / k_{r,\tau}$ (%)	$(k_{r,\tau} - k_{opt}) / k_{r,\tau}$ (%)
#1	0.381	0.378	0.280	0.79	26.5
#2	0.385	0.372	0.289	3.38	25.3
#3	0.397	0.382	0.290	3.79	26.8

thermal conductivity of the PVDF fibrous insulations increases from 0.280 to 0.821 mW m⁻¹ K⁻¹ as the temperature is increased from 300 to 420 K. The corresponding optimized diameter decreases from 2.0 to 1.7 μm. The mechanism was similar to the Rosseland mean extinction coefficient, which can be deduced by Eq. (6). Moreover, the radiative thermal conductivities could be obviously decreased by 25.9% and 17.2% at 300 and 420 K, respectively, by optimizing fiber diameters compared to that of experimental conditions.

Table 1 shows a comparison between radiative thermal conductivities ($k_{r,\tau}$) based on experimental measurements using Eq. (14) and those (k_r) based on the calculated optical constants using Eq. (6) for samples #1–#3. It could be observed that radiative thermal conductivities between $k_{r,\tau}$ and k_r had deviations of 0.79%, 3.38% and 3.79%, respectively. The slight deviations may be attributed to non-uniform distribution of fiber diameters and mixing of different crystalline owing to electrospinning instability. The

minimum radiative thermal conductivity (k_{opt}) of 0.28 mW m⁻¹ K⁻¹ could be obtained by optimizing fiber diameter of 2 μm at 300 K, which were 26.5%, 25.3% and 26.8% less than samples #1–3, respectively. This demonstrate an efficient method of predicting and optimizing thermal insulation performance of fibrous materials aiming to reducing heat loss and thermal energy conservation.

5. Conclusions

Based on experimental preparation and infrared spectral measurement of ultrafine PVDF fibers, spectral optical constants were obtained by using the Mie scattering theory, Beer’s law and SKK relation. This provided fundamental data to calculate thermal radiative conductivity of fibrous insulations. To ensure the uniqueness of solutions, the critical diameter of PVDF fibers was obtained with 1.06 μm. The effect of fiber diameter on thermal conductivity was investigated aiming at minimizing the radiative thermal conductivity. The optimized fiber diameter decreased from 2.0 to 1.7 μm and the corresponding minimum radiative thermal conductivity increased from 0.280 to 0.821 mW m⁻¹ K⁻¹ as the temperature was increased from 300 to 420 K. The optimized radiative thermal conductivity could be approximately 25% less than those of the experimental materials.

Acknowledgements

This research was supported by the Guangdong Province Natural Science Foundation for Distinguished Young Scientists, China (No. S2013050014139) and the Research Grant by Yangcheng Scholars Research Project of China (No. 1201561560).

References

- W.Q. Li, Z.G. Qu, Experimental study of effective thermal conductivity of stainless steel fiber felt, *Appl. Therm. Eng.* 86 (2015) 119–126.
- M.R. Wang, Q.J. Kang, N. Pan, Thermal conductivity enhancement of carbon fiber composites, *Appl. Therm. Eng.* 29 (2009) 418–421.
- S. Das, M. Bhowmick, S.K. Chattopadhyay, S. Basak, Application of biomimicry in textiles, *Curr. Sci.* 109 (2015) 893–901.
- M.R. Wang, N. Pan, Predictions of effective physical properties of complex multiphase materials, *Mater. Sci. Eng. R – Rep.* 63 (2008) 1–30.
- A. Andreozzi, N. Bianco, O. Manca, V. Naso, Numerical analysis of radiation effects in a metallic foam by means of the radiative conductivity model, *Appl. Therm. Eng.* 49 (2012) 14–21.
- N. Nima, M. Alexandre, Three dimensional radiative heat transfer model for the evaluation of the anisotropic effective conductivity of fibrous materials, *Int. J. Heat Mass Transf.* 83 (2015) 629–635.
- T.W. Tong, C.L. Tien, Radiative heat transfer in fibrous insulations – Part I: analytical study, *J. Heat Transf.* 105 (1983) 70–75.
- N. Nouri, Radiative Conductivity Analysis of Low-Density Fibrous Materials, Theses and Dissertations-Mechanical Engineering, Paper 66, 2015.
- R. Arambakam, H.V. Tafreshi, B. Pourdeyhimi, Modeling performance of multi-component fibrous insulations against conductive and radiative heat transfer, *Int. J. Heat Mass Transf.* 71 (2014) 341–348.
- J.M. Yang, H.J. Wu, S.Q. He, M.R. Wang, Prediction of thermal conductivity of fiber/aerogel composites for optical thermal insulation, *J. Porous Media* 18 (2015) 971–984.
- M.F. Modest, Radiative Heat Transfer, Academic Press, New York, 2013.
- A. Ahadi, M.Z. Saghir, An extensive heat transfer analysis using Mach Zehnder interferometry during thermodiffusion experiment on board the international space station, *Appl. Therm. Eng.* 62 (2014) 351–364.
- J. Ma, D.W. Sun, H. Pu, Spectral absorption index in hyperspectral image analysis for predicting moisture contents in pork longissimus dorsi muscles, *Food Chem.* 197 (2016) 848–854.
- L.M. Ruan, X.Y. Wang, H. Qi, S.G. Wang, Experimental investigation on optical constants of aerosol particles, *J. Aerosol Sci.* 42 (2011) 759–770.
- S.R. Bhattacharyya, R.N. Gayen, R. Paul, A.K. Pal, Determination of optical constants of thin films from transmittance trace, *Thin Solid Films* 517 (2009) 5530–5536.
- P. Gushterova, P. Sharlandjiev, Determination of optical constants (n, k, d) of very thin films deposited on absorbing substrate, *Vacuum* 76 (2004) 185–189.
- L.A. Dombrovsky, J.H. Randrianalisoa, D. Baillis, Infrared radiative properties of polymer coatings containing hollow microspheres, *Int. J. Heat Mass Transf.* 50 (2007) 1516–1527.
- L.M. Ruan, H. Qi, W. An, H.P. Tan, Inverse radiation problem for determination of optical constants of fly-ash particles, *Int. J. Thermophys.* 28 (2007) 1322–1341.

- [19] B. Ding, M.R. Wang, X.F. Wang, J.Y. Yu, G. Sun, Electrospun nanomaterials for ultrasensitive sensors, *Mater. Today* 13 (2010) 16–27.
- [20] M. Baqeri, M.M. Abolhasani, M.R. Mozdianfar, Q.P. Guo, A. Oroumei, M. Naebe, Influence of processing conditions on polymorphic behavior, crystallinity, and morphology of electrospun poly(Vinylidene fluoride) nanofibers, *J. Appl. Polym. Sci.* 132 (2015) 42304.
- [21] P. Frontera, C. Busacca, P. Antonucci, M.L. Faro, E. Falletta, C.D. Pina, D. Acierno, Polyaniline nanofibers: towards pure electrospun PANI, *AIP Conf. Proc. – Am. Inst. Phys.* 1459 (2012) 253–255.
- [22] H. Sadat, A general lumped model for transient heat conduction in one-dimensional geometries, *Appl. Therm. Eng.* 25 (2005) 567–576.
- [23] C.F. Bohren, D.R. Huffman, *Absorption and Scattering of Light by Small Particles*, Wiley, New York, 2008.
- [24] T. Xie, Y.L. He, Z.J. Hu, Theoretical study on thermal conductivities of silica aerogel composite insulating material, *Int. J. Heat Mass Transf.* 58 (2013) 540–552.
- [25] Y.L. He, T. Xie, Advances of thermal conductivity models of nanoscale silica aerogel insulation material, *Appl. Therm. Eng.* 81 (2015) 28–50.
- [26] R. Siegel, *Thermal Radiation Heat Transfer*, CRC press, Boca Raton, 2001.
- [27] M.E. Milham, R.H. Frickel, J.F. Embury, D.H. Anderson, Determination of optical constants from extinction measurements, *JOSA* 71 (1981) 1099–1106.
- [28] H.J. Wu, Y.T. Chen, Q.L. Chen, Y.F. Ding, X.Q. Zhou, H.T. Gao, Synthesis of flexible aerogel composites reinforced with electrospun nanofibers and microparticles for thermal insulation, *J. Nanomater.* 2013 (2013) 1–8.
- [29] L.M.M. Costa, R.E.S. Bretas, R. Gregorio, Effect of solution concentration on the electrospay/electrospinning transition and on the crystalline phase of PVDF, *Mater. Sci. Appl.* 1 (2010) 247–252.
- [30] H.J. Wu, J.T. Fan, X.H. Qin, G.G. Zhang, Thermal radiative properties of electrospun superfine fibrous PVA films, *Mater. Lett.* 62 (2008) 828–831.
- [31] E.D. Palik, *Handbook of Optical Constants of Solids*, San Diego, Academic Press, CA, 1998.
- [32] B.E.A. Saleh, M.C. Teich, B.E. Saleh, *Fundamentals of Photonics*, Wiley, New York, 1991.